

A central role for heme iron in colon carcinogenesis associated with red meat intake

Article

Accepted Version

Supplemental Material

Bastide, N., Chenni, F., Audebert, M., Santarelli, R., Tache, S., Naud, N., Baradat, M., Jouanin, I., Surya, R., Hobbs, D., Kuhnle, G. ORCID: <https://orcid.org/0000-0002-8081-8931>, Raymond-Letron, I., Gueraud, F., Corpet, D. and Pierre, F. (2015) A central role for heme iron in colon carcinogenesis associated with red meat intake. *Cancer Research*, 75 (5). pp. 870-879. ISSN 0008-5472 doi: <https://doi.org/10.1158/0008-5472.CAN-14-2554> Available at <https://centaur.reading.ac.uk/38674/>

It is advisable to refer to the publisher's version if you intend to cite from the work. See [Guidance on citing](#).

To link to this article DOI: <http://dx.doi.org/10.1158/0008-5472.CAN-14-2554>

Publisher: American Association for Cancer Research

All outputs in CentAUR are protected by Intellectual Property Rights law, including copyright law. Copyright and IPR is retained by the creators or other copyright holders. Terms and conditions for use of this material are defined in the [End User Agreement](#).

www.reading.ac.uk/centaur

CentAUR

Central Archive at the University of Reading

Reading's research outputs online

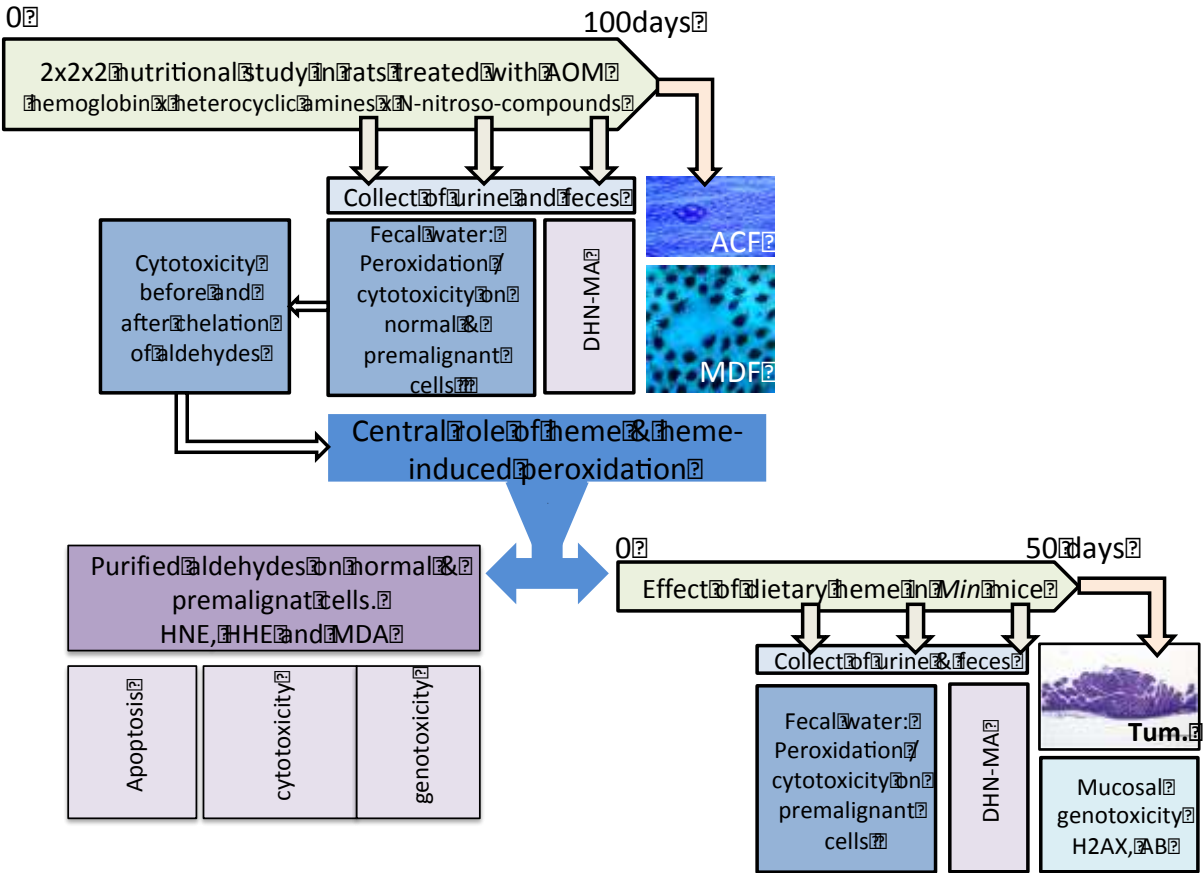
Supplementary Material

A central role for heme iron in colon carcinogenesis associated with red meat intake

Nadia Bastide ^{*1,4}, Fatima Chenni ^{*1}, Marc Audebert¹, Raphaëlle Santarelli¹, Sylviane Taché¹, Nathalie Naud¹, Maryse Baradat¹, Isabelle Jouanin¹, Reggie Surya¹, Ditte A Hobbs², Gunter G Kuhnle², Isabelle Raymond-Letron³, Françoise Gueraud¹, Denis Corpet¹, Fabrice Pierre ¹.

Correspondence to: f.pierre@toulouse.inra.fr

In this study the relative contribution of heme iron, heterocyclic amines and NOC to carcinogenesis was determined by a factorial design and preneoplastic endpoints in chemically-induced rats and validated on tumor endpoints in *Min* mice. The molecular mechanisms (genotoxicity, cytotoxicity, apoptosis) were analyzed *in vitro* in normal and preneoplastic cell lines and genotoxicity was confirmed on colon mucosa. The following flow chart (Supplementary Figure 1) resumed this study.



Supplementary Figure 1: Flowchart of Bastide et al.

Supplementary Materials and methods

Validation of the *Apc* $+/+$ and *Apc* $-/+$ Cell Lines

Immunofluorescence microscopy. The actin network is affected by the *Apc* mutation, so the presence or absence of the *Min* mutation was confirmed in both cell lines by observing the actin networks by immunofluorescence microscopy. Cells were seeded on glass coverslips and fixed in 2% formaldehyde in culture medium for 20 min. After three 5-min washes in PBS containing 1 mM CaCl₂ and 1 mM MgCl₂ (PBS+), cells were permeabilized with 0.05%/0.05% Triton X-100/Tween 20 in PBS+ for 3 min at RT. After three washes in PBS+, nonspecific binding sites were blocked by incubating the cells with 3% BSA in PBS+ for 30 min. The cell monolayer was incubated with rhodamine-labeled phalloidin (Sigma) to label the actin and with DAPI to label the nucleus. Imaging was performed using an Olympus BX60 fluorescence microscope.

Quantification of DNA and Counting the Number of Multinucleated Cells. To confirm that the *Apc* mutation induced genomic instability, we examined the effects of the mutation on the quantity of DNA and on the number of multinucleated cells. Trypsinized cells were washed twice by centrifugation for 5 min at 500 x g and resuspended in PBS. Absolute ethanol was added drop-wise while vortexing for a final ethanol concentration of 70%. Cells were fixed overnight at -20°C. Cells were then rehydrated by washing twice with PBS and resuspended in PBS plus 50 µg/ml propidium iodide, 100 µg/ml RNase (1:100 and 1:1000 of stock solutions, respectively). After incubation at 0°C in the dark for at least 30 min, cells were analyzed using a Coulter XL flow cytometer and Expo32 software (Beckman Coulter, France). The proportion of multinucleated cells was examined after DAPI staining. Imaging was performed on an Olympus BX60 fluorescence microscope.

Cytotoxicity Assays

MTT assay. Cells were seeded into 96-well culture plates at a seeding density of 5×10^3 cells per well in Dulbecco-modified essential medium (DMEM) supplemented with 10% (v/v) fetal calf serum, 1% (v/v) penicillin/streptomycin, and 10 U/mL interferon γ at the permissive temperature of 33°C. After 72 h, cells were transferred to 37°C without interferon γ for 24 h. Culture medium was replaced by culture medium without interferon γ and without fetal calf serum with added aldehydes at 2.5, 5, 10, 20, 40, and 80 μ M or with heme and 100 μ M fecal water. Untreated control wells were wells with culture medium without fetal calf serum and without interferon γ . After 24 h of incubation, cells were washed with PBS. Aldehyde cytotoxicity was quantified using 3-(4,5-dimethylthiazol-2-yl)-2,5 diphenyl tetrazolium bromide (MTT) at 0.9 mg/ml in PBS. The reaction product was solubilized in 100- μ l lysis buffer (10% SDS, 0.1M NaOH) before the color of the reaction product was quantified at 570 nm and 690 nm using a plate reader. The results are expressed as the percentage of dead cells relative to untreated wells. These assays were performed in triplicate.

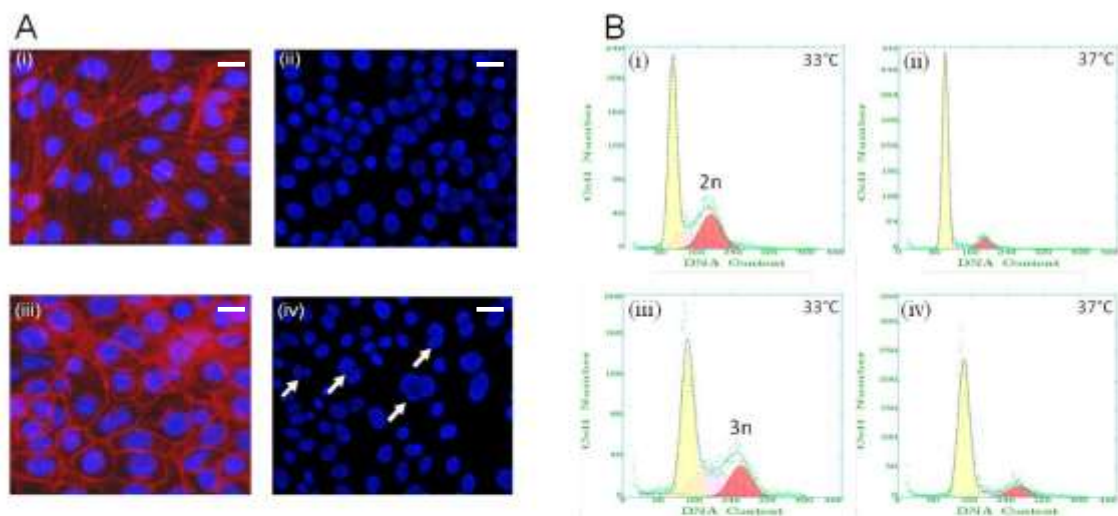
Luciferase-coupled ATP Quantification Assay. Cell viability was measured using a luciferase-coupled ATP quantification assay (CellTiter-Glo®; Promega). In this assay, the luminescent signal is proportional to the amount of ATP and consequently to the number of viable cells. At the end of treatment, 100- μ L of CellTiter-Glo® reagent was added and plates were shaken for 2 minutes on an orbital shaker. Plates were then incubated at RT for 10 min, and the luminescence intensity of each well was determined using an INFINITEM 200 plate reader (TECAN). The results are expressed as the percentage of dead cells relative to untreated wells. These assays were performed in triplicate.

Urinary assays

Urinary 1,4-dihydroxynonane mercapturic acid assay (DHN-MA). Urinary DHN-MA indicates the *in vivo* and in diet formation of 4-hydroxynonenal. The DHN-MA assay was performed by competitive enzyme immunoassay as described previously (Guéraud, 2006). Each urine sample was assayed in duplicate.

Supplementary Results

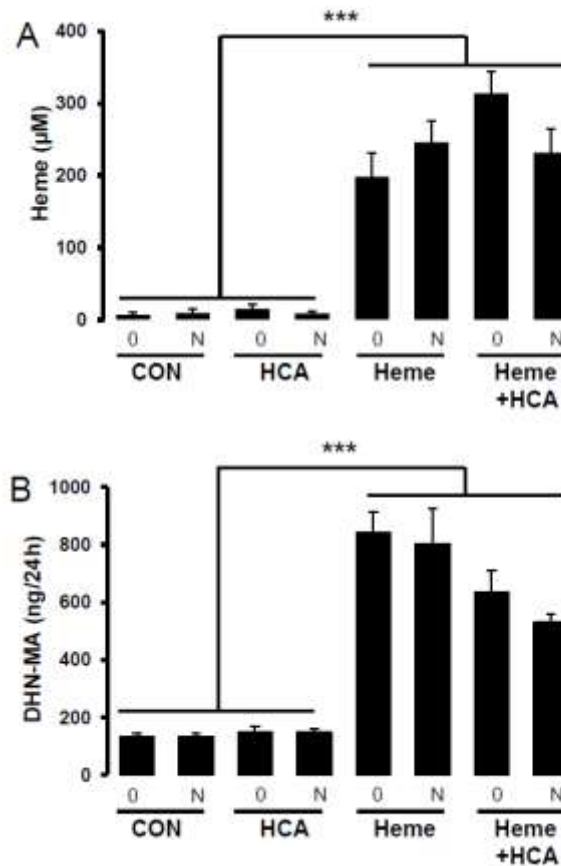
Apc Mutation Induces Resistance to Cytotoxicity Induced by Fecal Water from Heme-fed Rats in Premalignant Epithelial Cells: The Central role of Aldehydes



Supplementary Figure 2. The consequences of the loss of Apc function in an intestinal cellular model derived from C57BL/6J mice. (A) (Ai and Aiii) Disorganization of the actin cytoskeleton as seen by immunofluorescence staining of Apc^{+/+} (Ai) and Apc^{-/+} (Aiii) cells in the presence of phalloidin (confocal fluorescence microscopy). (Aii and Aiv) Accumulation of multinucleated cells. Apc^{+/+} (Aii) and Apc^{-/+} (Aiv) cells were fixed and stained with DAPI. Arrows indicate multinucleated cells. Scale bar: 20 μ m (B) Aneuploidy: cell cycle progression of Apc^{+/+} cells at 33°C (Bii); Apc^{+/+} cells at 37°C; Apc^{-/+} cells at 33°C (Biii); and Apc^{-/+} cells at 37°C (Biv).

As expected, the culture conditions affected cell proliferation due to the thermolabile tsA58 T antigen, which confers conditional immortalization. The percentage of cells in S phase decreased from 19.0% to 6.5% and from 29.7% to 9.4% for Apc +/+ and Apc -/+ cells, respectively, when the cells were transferred from 33°C to 37°C (**Supplementary Fig 2B**). Thus, the *in vitro* assays were performed at 37°C in order to mimic primary culture. However, we had to ensure that our cellular model showed the cellular changes that were expected as a consequence of the Apc mutation. As classically associated with mutation of the Apc gene loss of the Apc gene product led to disorganization of the integrity of the actin cytoskeletal as visualized by phalloidin (**Supplementary Fig 2Aiii**). In contrast, in Apc +/+ cells, the integrity of the actin cytoskeleton was preserved (**Supplementary Fig 2Ai**). Furthermore, previous research suggested that the Apc mutant dominantly induces aneuploidy and multinucleation of cells *in vivo*. As expected, evaluating the quantity of DNA showed that the Apc mutation induced polyploidy in the cellular model, with 1.5 times more DNA in mutated cells than in non-mutated cells (Fig. 2B). In agreement with this result and as expected, we observed that the Apc mutation was associated with a higher proportion of multinucleated cells in Apc -/+ cell culture (9.2±3.3%) compared to Apc +/+ cell culture (2.4±1.5%) (**Supplementary Fig 2Aii, Aiv**). These data confirmed that this cell model had the expected consequences of the Apc mutation.

One Hundred Day *In Vivo* Study of Azoxymethane-induced F344 rats: Demonstration of the Major Role of Heme Iron on Mucin-depleted Foci (MDF) Formation



Supplementary Figure 3. A diet with 1% hemoglobin results in increased heme in rat fecal water and in increased urinary biomarkers in rats. (A) Heme in fecal water. (B) A urinary biomarker of lipid peroxidation (DHN-MA). CON: control diet; HCA: diet with PhIP (50 $\mu\text{g}/\text{kg}$) and MeIQx (25 $\mu\text{g}/\text{kg}$); Heme: diet with 1% hemoglobin; Heme + HCA: diet with 1%hemoglobin, PhIP and MeIQx $2.39 \times 10^{-3}\%$; 0 drinking water control; N: drinking water with nitrites and nitrates at 0.34 g/l. Values are means \pm SEM; ***Significantly different from TEM and HCA, $p < 0.001$.

We found that diets containing hemoglobin significantly increased the levels of urinary 1,4-dihydroxynonemercapturic acid (DHN-MA), a metabolite of the lipid oxidation product 4-HNE (**Supplementary Fig 3B**). The level of this oxidation biomarker depended only on dietary and fecal heme (**Supplementary Fig 3A**) and remained unchanged when the diet contained nitrates/nitrites or heterocyclic amines without hemoglobin (**Supplementary Fig 3B**).

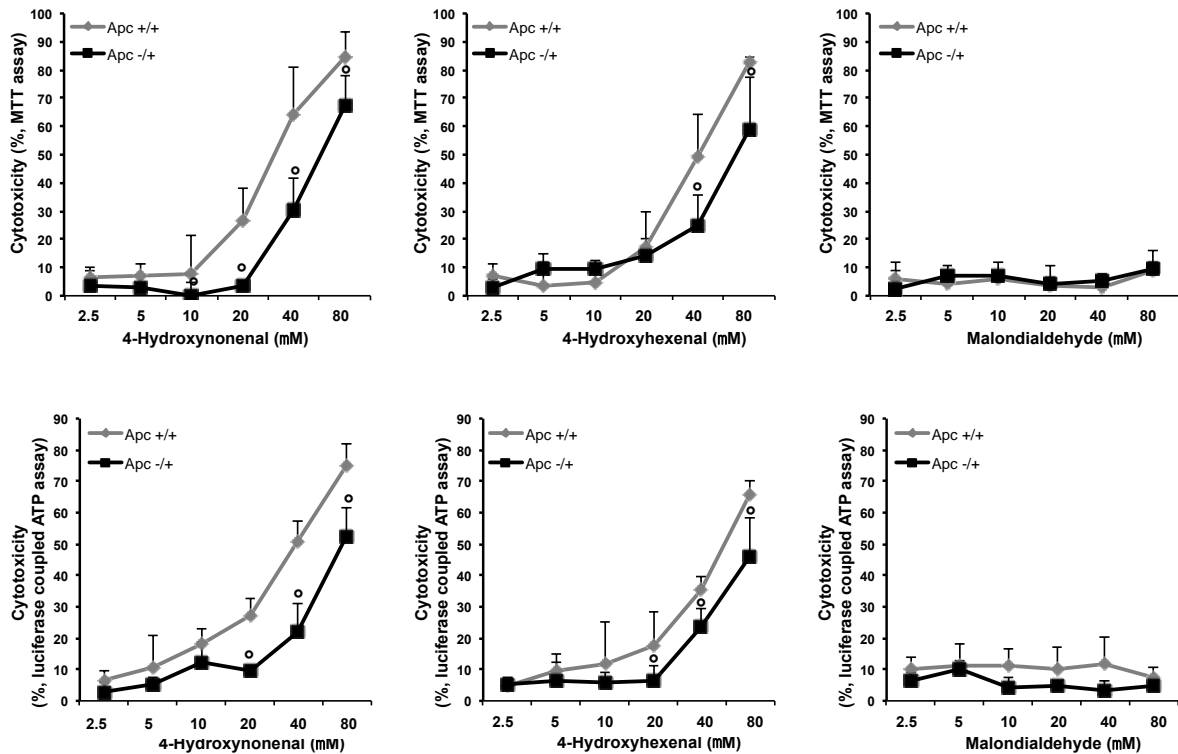
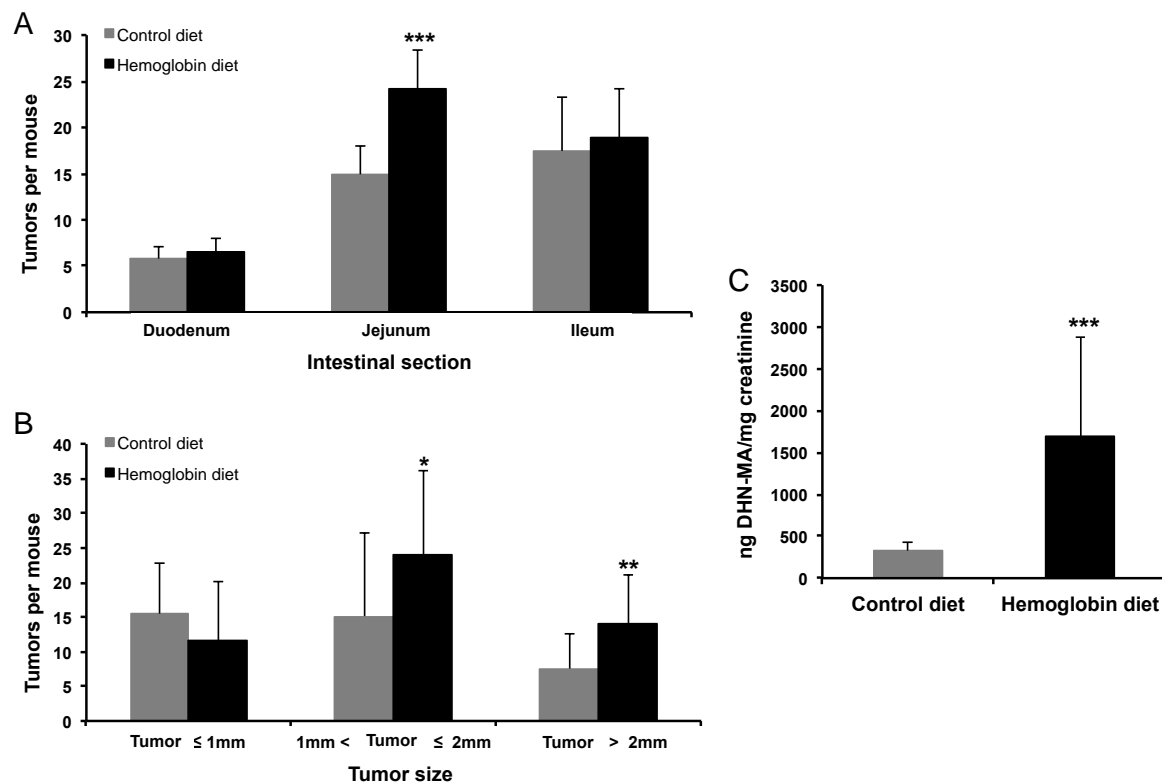


Fig.S2 Cytotoxic dose effect of aldehydes on Apc^{+/+} (grey line) and Apc^{-/+} (black line) cell lines

Supplementary Figure 4. The dose-dependent cytotoxic effects of HNE, MDA, and HHE on Apc^{+/+} cells (grey line) and Apc^{-/+} cells (black line) after 24 h of exposure. (A) MTT assay. (B) ATP quantification. All assays were performed in triplicate. Values are means \pm SEM. °Significantly different from Apc^{+/+} cells.

We confirmed the viability results with the MTT assay and the CellTiter-Glo® assay (**Supplementary Fig 4**), and we used a wider range of concentrations (0 to 80 μ M) in these assays. We confirmed that HNE and HHE were more cytotoxic (from 10 to 80 μ M and from 40 to 80 μ M, respectively) to normal cells than to preneoplastic ones, while MDA had no effect (**Supplementary Fig 4**).

Hemoglobin Increases Intestinal Tumorigenesis in *Apc*^{Min/+} Mice



Supplementary Figure 5. The effect of a hemoglobin diet on intestinal tumorigenesis in *Min* mice and modulation of a urinary biomarker linked to intestinal tumorigenesis. (A) The number of tumors per mouse according to intestinal section. (B) The number of tumors per mouse according to tumor size. (C) A urinary biomarker of lipid peroxidation (DHN-MA). Values are means ± SEM *Significantly different from control diet. (* $p < 0.05$; ** $p < 0.01$; *** $p < 0.001$).

The hemoglobin diet significantly increased the number of tumors in the jejunum (Supplementary Fig 5A). Considering the small intestine as a whole, the hemoglobin diet significantly increased the number of tumors with a diameter greater than 1 mm ($1 \text{ mm} < \text{tumor} \leq 2 \text{ mm}$, $p = 0.04$; $2 \text{ mm} < \text{tumor}$, $p = 0.006$) (Supplementary Fig 5B). As observed in rats, the effect of dietary heme on *Min* mouse tumors was associated with a significant increase in urinary DHN-MA (Supplementary Fig 5C).